

Clusterization Probability in ^{14}N Nuclei

N. Burtebayev, Sh. Hamada, Zh. Kerimkulov, D. K. Alimov, A. V. Yushkov, N. Amangeldi, A. N. Bakhtibaev

Abstract—The main aim of the current work is to examine if ^{14}N is candidate to be clusterized nuclei or not. In order to check this attendance, we have measured the angular distributions for ^{14}N ion beam elastically scattered on ^{12}C target nuclei at different low energies; 17.5, 21, and 24.5 MeV which are close to the Coulomb barrier energy for $^{14}\text{N}+^{12}\text{C}$ nuclear system. Study of various transfer reactions could provide us with useful information about the attendance of nuclei to be in a composite form (core + valence). The experimental data were analyzed using two approaches; Phenomenological (Optical Potential) and semi-microscopic (Double Folding Potential). The agreement between the experimental data and the theoretical predictions is fairly good in the whole angular range.

Keywords—Deuteron Transfer, Elastic Scattering, Optical Model, Double Folding, Density Distribution.

I. INTRODUCTION

THE study of nuclear reaction is of special importance as it could provide us with useful information about nuclear structure, spectroscopic amplitude, asymptotic normalization coefficient, deformation parameters, transition probability etc. There are some nuclear systems such as $^{16}\text{O}+^{12}\text{C}$ at low energies showed a remarkable increase in differential cross sections at backward angles which have been interpreted to be mainly due to the contribution of alpha cluster transfer. Consequently ^{16}O nuclei is well known to be clusterized nuclei, it could be treated as a composite nuclei consisting of (^{12}C Core) and (Alpha particle Valence). On the other hand, if ^{14}N is candidate to be clusterized nuclei in the form of (^{12}C Core) and (deuteron Valence), so we should observe an increase in the differential cross sections at backward angles which could be interpreted to be due to deuteron transfer. There have been rather extensive measurements for $^{14}\text{N}+^{12}\text{C}$ nuclear system [1]–[6]. The angular distribution measurements for $^{12}\text{C}(^{14}\text{N}, ^{14}\text{N})^{12}\text{C}$ at $E(^{14}\text{N})=78$ MeV performed by W. von Oertzen et al. [1] and also the measurements performed by Isao Kohno et al. [2] in the energy range 49.3 – 83.5 MeV weren't extended enough upto large angles to observe the effect of deuteron transfer. While, the experimental

measurements performed at the Erlangen tandem accelerator by Helb et al. [3] at $E_{\text{lab}}=22.5$ MeV showed that there is a slight increase in differential cross section at back ward angles. It's well known that such transfer reaction could be observed at low energies, so we have studied $^{14}\text{N}+^{12}\text{C}$ elastic scattering at low energies; 17.5, 21, and 24.5 MeV which are close to the Coulomb barrier energy for this nuclear system. At relatively high energy 20 MeV/A [4] the measurements of differential cross section for ^{14}N scattered on ^{12}C target nuclei displayed a Fraunhofer crossover followed by a structure less falloff. The experimental measurements for $^{14}\text{N}+^{12}\text{C}$ at $E_{\text{lab}}=21.34$ MeV [5] showed oscillatory structures in the angular distributions which has been interpreted to be due to exchange of the mass difference of the two colliding nuclei.

II. EXPERIMENTAL DETAILS

The experimental measurements for $^{14}\text{N}+^{12}\text{C}$ nuclear system were performed in the cyclotron DC-60 located in Institute of Nuclear Physics National Nuclear Center, Almaty-Kazakhstan (INP NNC RK). The ^{14}N ion beam has been accelerated up to energies 1.25, 1.5, and 1.75 MeV/n and then directed to ^{12}C target nuclei of thickness $31.9 \mu\text{g}/\text{cm}^2$. The beam current was nearly equal to 20 nA during these experiments, the angular distribution was measured in a wide range of angles $\approx 20\text{--}130^\circ$ in center of mass system. Energy spectra of scattered particles were recorded with a semiconductor silicon surface barrier detector ORTEC company sensitive layer with a thickness of 100 microns. The energy resolution of the registration system was 250–300 keV, which is mainly determined by the energy spread of the primary beam. Only one detector was used in our measurements which detect both ^{14}N fragment and ^{12}C residual peaks. Spectrum analysis has been performed using program MAESTRO [7]. The spectrum files showed two peaks, one is corresponding to ^{14}N and the other for ^{12}C . Fig. 1 shows the spectrum for $^{12}\text{C}(^{14}\text{N}, ^{14}\text{N})^{12}\text{C}$ elastic scattering at angle 45° and at energy 24.5 MeV.

The ^{12}C target with thickness of $\sim 32 \mu\text{g}/\text{cm}^2$ was prepared using the technique of vacuum evaporation by resistance heating of the specimen with a spot electron gun at the facility UVS-2 (universal vacuum system) see Fig. 2. The preparation chamber was connected with two pumps; rotary pump and turbo molecular pump to achieve the desired vacuum (2×10^{-6} torr) inside the chamber. Firstly, we deposited layers of NaCl crystal salt onto glass plates with the aid of tantalum cradle. Then, electron gun is directed to a sample of graphite with ^{12}C concentration of 98% and placed 3 cm from the electron gun. The size of the beam spot (2–3 mm diameter). Under the influence of electrons, the sample is strongly heated, evaporated, and deposited onto glass plates with previously deposited layers of salt which acts as a release agent and

N. Burtebayev is with the Institute of Nuclear Physics, Almaty, Kazakhstan (e-mail: nburtebayev@yandex.ru).

Sh. Hamada is with Faculty of Science, Tanta University, Tanta, Egypt (e-mail: sh.m.hamada@gmail.com).

Zh. Kerimkulov is with the Institute of Nuclear Physics, Almaty, Kazakhstan (e-mail: zhambul-k@yandex.ru).

D. K. Alimov is with Al-Farabi Kazakh National University, Almaty, Kazakhstan (e-mail: diliyo@mail.ru).

A. V. Yushkov is with Al-Farabi Kazakh National University, Almaty, Kazakhstan.

N. Amangeldi is with L. N. Gumilev Eurasia National University, Astana, Kazakhstan (e-mail: nur19792@mail.ru).

A. N. Bakhtibaev is with Ahmet Yassawy International Kazakh-Turkish University, Turkistan, Kazakhstan.

facilitates the removal of carbon film. After annealing for 12 hours at 150°C, the carbon films were removed from the glass plates and placed to specially prepared frames.

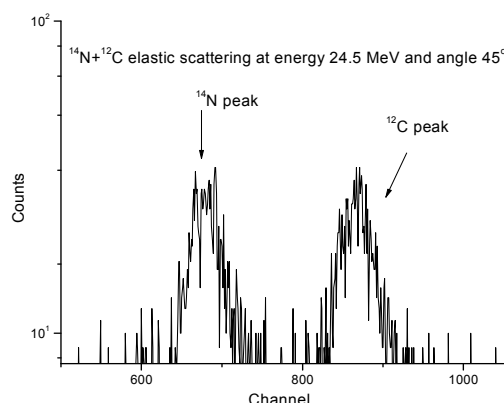


Fig. 1 Spectrum for $^{12}\text{C}(^{14}\text{N}, ^{14}\text{N})^{12}\text{C}$ elastic scattering at angle 45° and at energy 24.5 MeV

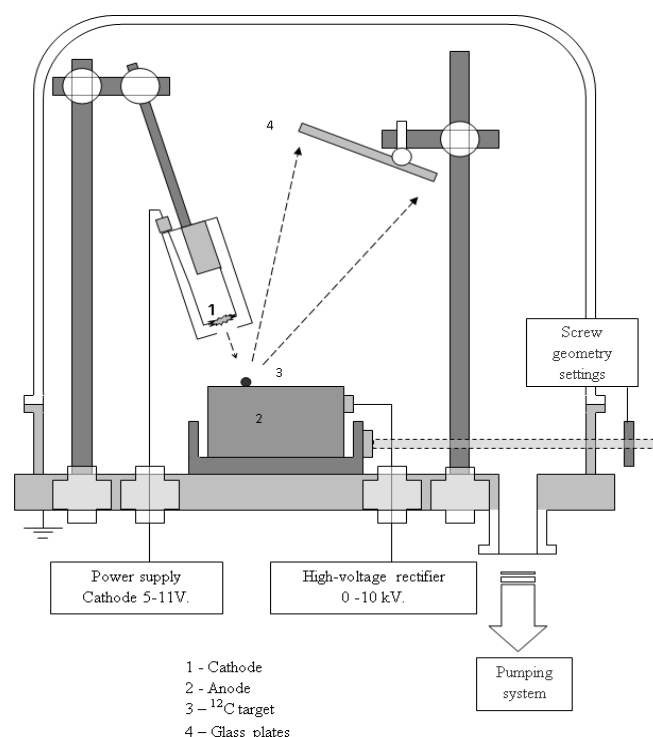


Fig. 2 Block diagram for the device used for the deposition of ^{12}C on glass plates using electron gun

The determination of the target thickness was carried out using reactions that have narrow and well isolated resonances. For this purpose, the reactions $^{27}\text{Al}(p, \gamma)^{28}\text{Si}$ at $E_{p, \text{lab}} = 992 \text{ keV}$ [8] was used. To register, the resulting gamma-ray, HpGe detector GEM 20P was used with high energy resolution (1-2 keV). After the measurement of the target yield curves over the $^{27}\text{Al}(p, \gamma)^{28}\text{Si}$ resonance at $E_p = 992 \text{ keV}$ (which has a total width of 0.10 keV) for an aluminum foil and the target with the Al film is made, target thickness is taken from the shift of the resonance energy obtained by comparing these yield

curves as shown in Fig. 3. Then stopping power tables [9] are used to obtain the atomic density of the studied isotope film. This method allows determining thicknesses of films in the 10 – 100 $\mu\text{g}/\text{cm}^2$ range with an uncertainty less than 5%.

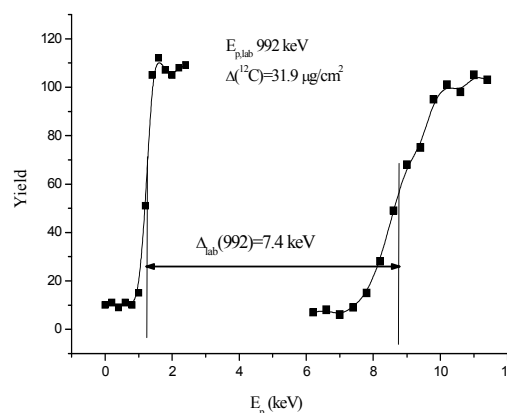


Fig. 3 The shift of the 992 keV resonance energy of the $^{27}\text{Al}(p, \gamma)^{28}\text{Si}$ reaction at the presence of the carbon film. The thickness of the ^{12}C target is $31.9 \mu\text{g}/\text{cm}^2$

III. THEORETICAL CALCULATIONS

The elastic scattering process between two nuclei can be described by finding a solution of the Schrödinger's equation $H\Psi = E\Psi$, or equivalently:

$$\left[-\frac{\hbar^2}{2\mu} \nabla^2 + V(r) \right] \Psi(r) = E\Psi(r) \quad (1)$$

where μ represents the reduced mass of the system. The potential $V(r)$ is generally composed of a Coulomb and a complex nuclear potential. The wave function $\Psi(r)$ is a sum of the incoming plane wave and the outgoing spherical wave

$$\Psi(r) = A_0 \left(\exp(i\vec{k} \cdot \vec{r}) + f(\theta, \varphi) \frac{\exp(ikr)}{r} \right) \quad (2)$$

where $f(\theta, \varphi)$ is the scattering amplitude and \vec{k} is the wave number of the incoming wave. The differential scattering cross section is related to the scattering amplitude by $\frac{d\sigma}{d\Omega} = |f(\theta, \varphi)|^2$. Due to the effects of both electromagnetic and nuclear interactions, the total scattering amplitude could be written as $f(\theta, \varphi) = f_C(\theta) + f_N(\theta, \varphi)$ and therefore, the differential cross section for the elastic scattering between to nuclei is expressed in the form

$$\frac{d\sigma}{d\Omega}(\theta, \varphi) = |f_C(\theta) + f_N(\theta, \varphi)|^2 \quad (3)$$

The Coulomb amplitude is written as

$$f_C(\theta) = -\frac{\eta}{2k \sin^2\left(\frac{\theta}{2}\right)} \exp\left[-i\left(\eta \ln\left(\sin^2\left(\frac{\theta}{2}\right)\right) + 2\sigma_0\right)\right] \quad (4)$$

where the scattering amplitude of the nuclear interaction is given by

$$f_N(\theta, \varphi) = \frac{1}{2ik} \sum_l (2l+1) \exp(2i\sigma_l) [S_l - 1] P_l(\cos \theta) \quad (5)$$

$P_l(\cos \theta)$ are the Legendre polynomials, and S_l represents the unitary scattering matrix which is expressed in terms of the reflection coefficients A_l and the scattering phase shifts δ_l .

$$S_l = A_l \exp(2i\delta_l) \quad (6)$$

The data on elastic scattering were analyzed within the framework of the standard optical model (OM) of the nucleus, where the influence of non-elastic channels is taken into account by introducing a phenomenological imaginary absorptive part in the interaction potential between the colliding nuclei. In this model the elastic scattering is often described by a complex interaction potential with a radial dependence in the form of Woods-Saxon. Parameters of optical potential (OP) were selected to achieve the best agreement between theoretical and experimental angular distributions. Woods-Saxon form factor was taken for both the real and imaginary parts of the potential.

$$U(r) = V_0 \left[1 + \exp\left(\frac{r - R_V}{a_V}\right) \right]^{-1} + iW \left[1 + \exp\left(\frac{r - R_W}{a_W}\right) \right]^{-1} \quad (7)$$

Coulomb potential of a uniform charged sphere

$$V_C(r) = \frac{Z_p Z_t e^2}{2R_C} \left(3 - r^2 / R_C^2 \right) \text{ for } r \leq R_C \quad (8)$$

$$V_C(r) = \frac{Z_p Z_t e^2}{r}, \text{ for } r > R_C$$

with radius $R_i = r_i (A_p^{1/3} + A_t^{1/3})$, $i = V, W, C$

The double folding (DF) calculations were performed using code DFMSPH [10]. In the double folding calculations, the real part of the potential is calculated from a more fundamental basis by the double folding method in which the NN interaction $V_{NN}(r)$, is folded into the densities of both the projectile and target nuclei

$$V^{DF}(R) = N_r \int \rho_t(r_2) \rho_p(r_1) V_{NN}(|R + r_2 - r_1|) d^3 r_1 d^3 r_2 \quad (9)$$

where N_r is a free renormalization factor, $\rho_p(r_1)$ and $\rho_t(r_2)$ are the nuclear matter density distributions of both the projectile and target nuclei, respectively, and $V_{NN}(|R + r_2 - r_1|)$ is the

effective NN interaction potential and it was taken to be of the CDM3Y6 form based on the M3Y-Paris potential:

$$v_D(s) = 11061.625 \frac{\exp(-4s)}{4s} - 2537.5 \frac{\exp(-2.5s)}{2.5s},$$

$$v_{EX}(s) = -1524.25 \frac{\exp(-4s)}{4s} - 518.75 \frac{\exp(-2.5s)}{2.5s} - 7.8474 \frac{\exp(-0.7072s)}{0.7072s} \quad (10)$$

The M3Y-Paris interactions are scaled by an explicit density-dependent function $F(\rho)$:

$$v_{D(EX)}(\rho, s) = F(\rho) v_{D(EX)}(s), \quad (11)$$

where $v_{D(EX)}$ are the direct and exchange components of the M3Y-Paris and ρ is the nuclear matter (NM) density. $F(\rho)$ was taken to be exponential dependence, and the parameters were adjusted to reproduce the NM saturation properties in the HF calculation.

The density-dependent function can be written as

$$F(\rho) = C[1 + \alpha \exp(-\beta\rho) - \gamma\rho^n], \quad (12)$$

the parameters C, α, β, γ listed in Table I were taken from [11].

TABLE I
PARAMETERS OF DENSITY-DEPENDENCE FUNCTION $F(\rho)$

Interaction Model	c	α	β (fm ³)	γ (fm ³ⁿ)	n	K (MeV)
CDM3Y6	0.2658	3.8033	1.4099	4.0	1	252

The density distribution of ^{12}C is expressed in a modified form of the Gaussian shape as $\rho(r) = \rho_0(1 + wr^2) \exp(-\beta r^2)$, where $\rho_0 = 0.1644$, $w = 0.4988$ and $\beta = 0.3741$ [12]. The ^{14}N density distribution was calculated using Modified Harmonic Oscillator (MHO), where $\rho(r)$ is expressed in the following form [13]:

$$\rho(r) = \rho_0 \left(1 + \alpha \left(\frac{r}{a} \right)^2 \exp\left(-\left(\frac{r}{a}\right)^2\right) \right), \quad (13)$$

$$\alpha = 1.234, a = 1.76, \rho_0 = 0.1428$$

The imaginary part of the potential was taken in the form of standard Woods-Saxon form factor. So, the nuclear potential in this case has the following shape:

$$U(R) = N_r V^{DF}(R) + iW(R) \quad (14)$$

IV. RESULTS AND DISCUSSION

Our measured experimental data at energies 17.5, 21 and 24.5 MeV and the previously measured data for $^{14}\text{N} + ^{12}\text{C}$ at energies 21.34 and 27.3 MeV [5] are presented in Fig. 4. It is clearly shown that our data at energy 21 MeV is so close to the

previously measured data at 21.34 MeV which emphasize that our data was measured correctly. Although the data at energies 21.34 and 27.3 MeV were extended to large angles than those measured by us, but these data don't show a significant increase in differential cross section at backward angles. The observed oscillatory structure at energies 21.34 and 27.3 MeV could be interpreted to be due to deuteron transfer between the interacting nuclei.

The comparisons between the experimental data and the theoretical predictions performed using both OM and DF approaches for $^{14}\text{N}+^{12}\text{C}$ nuclear system at energies 1.25, 1.5 and 1.75 MeV/n are shown in Figs. 5, 6 and 7 respectively. The measurements were not extended behind $\approx 130^\circ$, the data in this angular range doesn't show a significant increase in differential cross section at backward angles due to deuteron transfer. The agreement between the experimental and theoretical calculations is fairly good over the whole angular range using both OM and DF approaches. The obtained normalization factor (N_r) at the three concerned energies in this study (17.5, 21, 24.5 MeV) is in the range 1.0 - 1.152. Optimal optical potential parameters for $^{14}\text{N}+^{12}\text{C}$ nuclear systems, also those from double folding are listed in Table II.

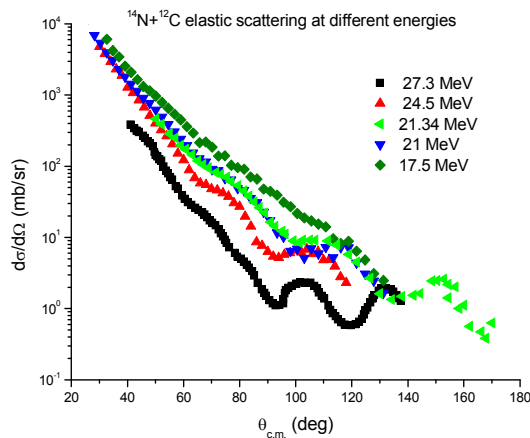


Fig. 4 Experimental angular distributions for $^{14}\text{N}+^{12}\text{C}$ elastic scattering at different energies: 17.5, 21, and 24.5 MeV (our data), 21.34 and 27.3 MeV from ref. [5])

TABLE II

OPTICAL POTENTIAL PARAMETERS USED IN THE OM ANALYSIS FOR THE ELASTIC SCATTERING $^{14}\text{N}+^{12}\text{C}$ NUCLEAR SYSTEM AT ENERGIES 17.5, 21 AND 24.5 MeV. FOLDING PARAMETERS WITH NORMALIZATION COEFFICIENT N_r ARE ALSO LISTED

E_{lab} MeV	Mode	V_0 MeV	r_v (fm)	a_v (fm)	W_0 MeV	r_w (fm)	a_w (fm)	N_r
17.5	OM	89.93	1.194	0.649	4.238	1.3	1.147	1.0
	DF				4.238	1.3	1.147	
21	OM	89.02	1.194	0.536	6.279	1.3	0.399	1.134
	DF				6.279	1.3	0.399	
24.5	OM	75.81	1.194	0.489	20.0	1.3	0.215	1.152
	DF				20.0	1.3	0.217	

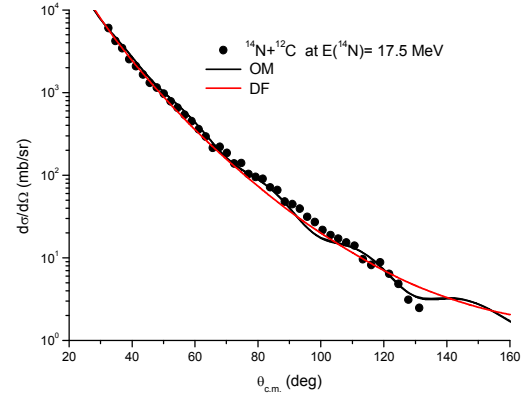


Fig. 5 Comparison between experimental and calculated differential cross section within the framework of OM and DF for ^{14}N elastically scattered by ^{12}C at energy 17.5 MeV

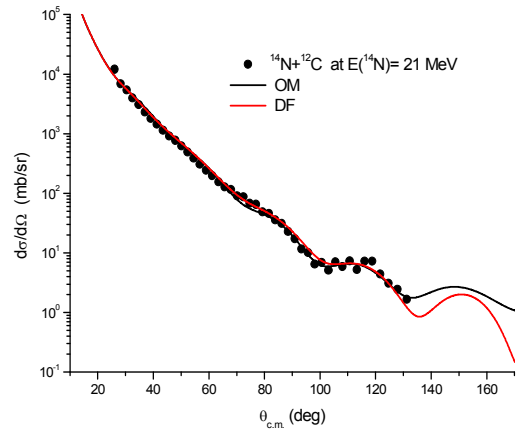


Fig. 6 Same as Fig. 5 but for energy 21 MeV

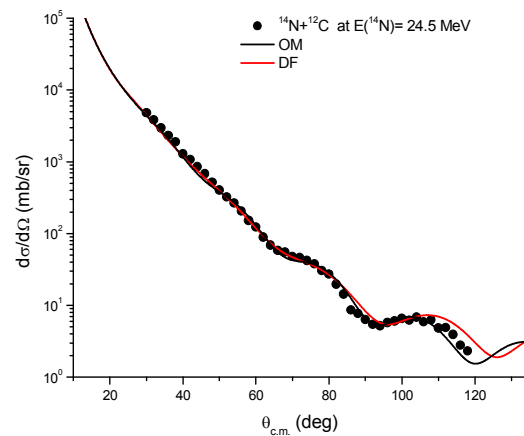


Fig. 7 Same as Fig. 5 but for energy 24.5 MeV

V. CONCLUSIONS

We have measured the angular distribution for ^{14}N elastically scattered on ^{12}C target nuclei at low energies close to Coulomb barrier energy for this nuclear system to examine if there will be any significant increase in differential cross sections at backward angles due to deuteron transfer. If such

transfer is well exist it means that ^{14}N nuclei is candidate to be clusterized nuclei.

It is clearly shown from our experimental data and the performed theoretical calculations that deuteron transfer doesn't play a significant role in the formation of differential cross section at backward angles but we can't neglect the effect of transfer in displaying the oscillatory structure observed in the experimental data measured at relatively low energies close to the Coulomb barrier energy for $^{14}\text{N}+^{12}\text{C}$ nuclear system, which testifies to a low clustering in the Nitrogen nucleus.

REFERENCES

- [1] W. Von Oertzen, M. Liu, C. Caverzasio, J. C. Jacmart, F. Pougheon, M. Riou, J. C. Roynette and C. Stephan, Nucl. Phys. A143, 34 (1970).
- [2] Isao Kohno, Shyunji Nakajima, Tadao Tonuma and Masatoshi Odera, Phys. Soc. Japan 30, 910 (1971).
- [3] H. D. Helb, H. Voit, G. Ischenko, and W. Reichardt, Phys. Rec. Lett. 23 (1969).
- [4] M. E. Brandan, S. E. Soberano, E. Belmont-Moreno, and A. Menchaca-Rocha, Phys. Rev. C42, 2236 (1990).
- [5] M. L. Halbert, C. E. Hunting and A. Zucker, Phys. Rev. 1117 (1960) 1545.
- [6] H. Amakawa and K. I. Kubo, Nucl. Phys. A266(1976).
- [7] MAESTRO®-32 MCA Emulator for Microsoft® Windows® 98, 2000, NT®, and XP® A65-B32 Software // User's Manual Software Version 6.
- [8] J.W. Bulter, Table of (p, γ) Resonances by Proton Energy: E = 0.163 – 3.0 MeV, U.S. Naval Research Laboratory. NRL Report. 5282 (1959).
- [9] Andersen H.H., Ziegler J.F. Hydrogen-Stopping Powers and Ranges in all elements. – Oxford: Pergamon Press, 1977.
- [10] I. I. Gontchar, M. V. Chushnyakova Computer Physics Communications 181 (2010) 168–182.
- [11] Khoa Dao T., Satchler G.R., von Oertzen W. Phys. Rev. C56 (1997) 954.
- [12] S. Qing-biao, F. Da-chun, Z. Yi-zhong, Phys. Rev. C 43 (1991) 2773.
- [13] C. W. De Jager, H. De Vries, and C. De Vries Atomic Data and Nuclear Data Tables 14, 479-508 (1974).